

Reduction of $1/f$ noise in graphene after electron-beam irradiation

Md. Zahid Hossain,¹ Sergey Rumyantsev,^{2,3} Michael S. Shur,²
 and Alexander A. Balandin^{1,4,a)}

¹Nano-Device Laboratory, Department of Electrical Engineering, Bourns College of Engineering,
 University of California–Riverside, Riverside, California 92521, USA

²Center for Integrated Electronics and Department of Electrical, Computer, and Systems Engineering,
 Rensselaer Polytechnic Institute, Troy, New York 12180, USA

³Ioffe Physical-Technical Institute, The Russian Academy of Sciences, St. Petersburg 194021, Russia

⁴Materials Science and Engineering Program, University of California–Riverside, Riverside,
 California 92521, USA

(Received 25 January 2013; accepted 9 April 2013; published online 19 April 2013)

We investigated experimentally the effect of the electron-beam irradiation on the level of the low-frequency $1/f$ noise in graphene devices. It was found that $1/f$ noise in graphene reduces with increasing concentration of defects induced by irradiation. The increased amount of structural disorder in graphene under irradiation was verified with micro-Raman spectroscopy. The bombardment of graphene devices with 20-keV electrons reduced the noise spectral density, S_I/I^2 (I is the source-drain current) by an order-of magnitude at the radiation dose of $10^4 \mu\text{C}/\text{cm}^2$. We analyzed the observed noise reduction in the limiting cases of the mobility and carrier number fluctuation mechanisms. The obtained results are important for the proposed graphene applications in analog, mixed-signal, and radio-frequency systems, integrated circuits and sensors. © 2013 AIP Publishing LLC [<http://dx.doi.org/10.1063/1.4802759>]

The level of the flicker $1/f$ noise¹ is one of the key metrics that each new material has to pass before it can be used for practical devices (f is the frequency).² Graphene³ has shown a great potential for applications in high-frequency communications,^{4,5} analog circuits,⁶ and sensors.^{7,8} The envisioned applications require a low level of $1/f$ noise, which contributes to the phase-noise of communication systems² and limits the sensor sensitivity.⁷ Despite significant research efforts^{9–15} there is still no conventionally accepted model for physical mechanisms behind $1/f$ noise in graphene. Correspondingly, no comprehensive methods for $1/f$ noise suppression in graphene devices have been developed.

In this letter, we show that $1/f$ noise in graphene reveals an interesting characteristic—it reduces with increasing concentration of defects induced by irradiation. We found that bombardment of graphene devices with 20-keV electrons can reduce the noise spectral density, S_I/I^2 (I is the source-drain current) by an order-of magnitude at the radiation dose (RD) of $10^4 \mu\text{C}/\text{cm}^2$. We analyzed the observed noise reduction in the framework of the mobility and carrier number fluctuation mechanisms. We hope that our experimental results can stimulate a detailed theoretical study of $1/f$ noise origin in graphene. Apart from contributing to understanding the physics behind $1/f$ noise in graphene, our results can possibly offer a practical method for noise reduction in various graphene devices where a trade-off between the noise level and mobility value is possible.

Graphene revealed a number of unique electronic,^{3–7} optical,⁷ and thermal¹⁶ properties, which led to proposals of different graphene-based devices. The high-frequency communication and analog circuit applications are expected to capitalize on high electron mobility and saturation velocity of

graphene.⁷ The ultimate surface-to-volume ratio and the Fermi-energy tuning capability make graphene excellent material for detectors and sensors with demonstrated single-molecule sensitivity⁷ and selective gas sensing.⁸ However, like with any other new material systems, graphene has to meet the stringent requirements for the low-frequency $1/f$ noise level.² For example, recent development of GaN technology for radio-frequency and optical communications required substantial decrease of the $1/f$ noise in this material.^{2,17}

A number of research groups have studied low-frequency noise in graphene devices.^{9–15} The noise spectral density, S_I/I^2 , follows $1/f$ law but reveals the gate-bias dependence different from that in semiconductor field-effect transistors.^{9–15} The noise level was reported to be smaller in bilayer,⁹ suspended,¹³ graded-thickness few-layer, and multi-layer graphene.¹⁴ Other reports pointed out that graphene is uniquely distinct from metals and semiconductors and a new framework is necessary to understand $1/f$ noise near the zero-carrier density.^{18–20} Specifically, it was suggested that the carrier-number fluctuation model is inadequate to understand the zero-carrier density limit in which the conductivity is proportional not to the carrier density, but to RMS deviations of the carrier density about zero.²¹ One should note here that there are many different mechanisms that can contribute to the current fluctuations including charged impurities, non-resonant short-range and resonant defect scatterers.^{21–24} In many experimental studies of $1/f$ noise in graphene, the interpretations of measured results were different. As of today, there is no commonly accepted model of $1/f$ noise in graphene, which could be used for various gating and environmental conditions. We undertook the present investigation considering that the irradiation experiments were crucial for gaining understanding $1/f$ noise in conventional materials and metal-oxide-semiconductor field-effect transistors.^{25–27} The study of the effects produced by the

^{a)}Author to whom correspondence should be addressed. Electronic mail: balandin@ee.ucr.edu.

electron beams on $1/f$ noise in graphene can elucidate the mechanisms of $1/f$ noise and answer a question of graphene's prospects for radiation-hard applications.

Graphene is relatively susceptible to the electron and ion bombardment owing to its single-atom thickness.^{28–30} Electron irradiation can introduce different types of defects in graphene depending on the beam energy and local environment, e.g., the presence of organic contaminants. For this study, we selected the electron energy of 20 keV in order to exclude the severe knock-on damage to the graphene crystal lattice, which starts at ~ 50 keV.³⁰ The back-gated graphene devices were fabricated using mechanical exfoliation⁵ and standard lithographic fabrication techniques.^{10,14} The number of atomic planes and absence of defects in pristine graphene have been checked with Raman spectroscopy. The devices were subjected to the electron-beam irradiation in the scanning-electron microscopy (SEM) chamber of the electron-beam lithography (EBL) system under high-vacuum conditions. The following testing protocol was applied. The Raman spectrum and $1/f$ noise were measured for all devices before irradiation. The graphene channels were then exposed to the first RD followed by the Raman spectroscopy and noise measurements. The process was repeated several times until the total RD reached $10^5 \mu\text{C}/\text{cm}^2$.

Figure 1(a) shows a SEM image of a graphene channel with four metal contacts, while Figure 1(b) illustrates the area of graphene between two contacts subjected to irradiation.

The Raman spectrum of graphene before and after irradiation with $\text{RD} = 10^4 \mu\text{C}/\text{cm}^2$ is presented in Figure 1(c). One can see the appearance of the strong disorder D and D' peaks after irradiation indicating that electron bombardment introduced defects to graphene.²⁹ The strength of the irradiation effects can be deduced from the intensity ratio, $I(D)/I(G)$, presented in Figure 1(d). $I(D)/I(G)$ increases monotonically with RD in the range of interest. Defect introduction results in corresponding asymmetric broadening of 2D band, which can also be used to monitor defects introduction (see inset in Figure 1(d)).

The electrical conduction properties of graphene under irradiation evolved as we expected. The electron bombardment led to a shift in the Dirac point position and decrease in mobility, μ , with the corresponding increase in the source-drain resistance, R_{SD} . The initial position of the Dirac point ($V_D \sim 10$ V) is typical for as-fabricated devices owing to the background doping from water moisture or resist residues from lithographic processes. The Dirac point shifted to ~ 2 V after exposure to $\text{RD} = 10^4 \mu\text{C}/\text{cm}^2$ (Figure 2(a)). Such a behavior was observed for most devices, although in a very few cases, we recorded a positive shift of the Dirac point after some irradiation steps. The mobility decreases with increasing RD but remains acceptable from the applications point of view (Figure 2(b)). The low-frequency noise measurements were performed using the in-house built setup shielded inside a metal enclosure. The noise was measured in the linear region of the drain bias keeping the source at a

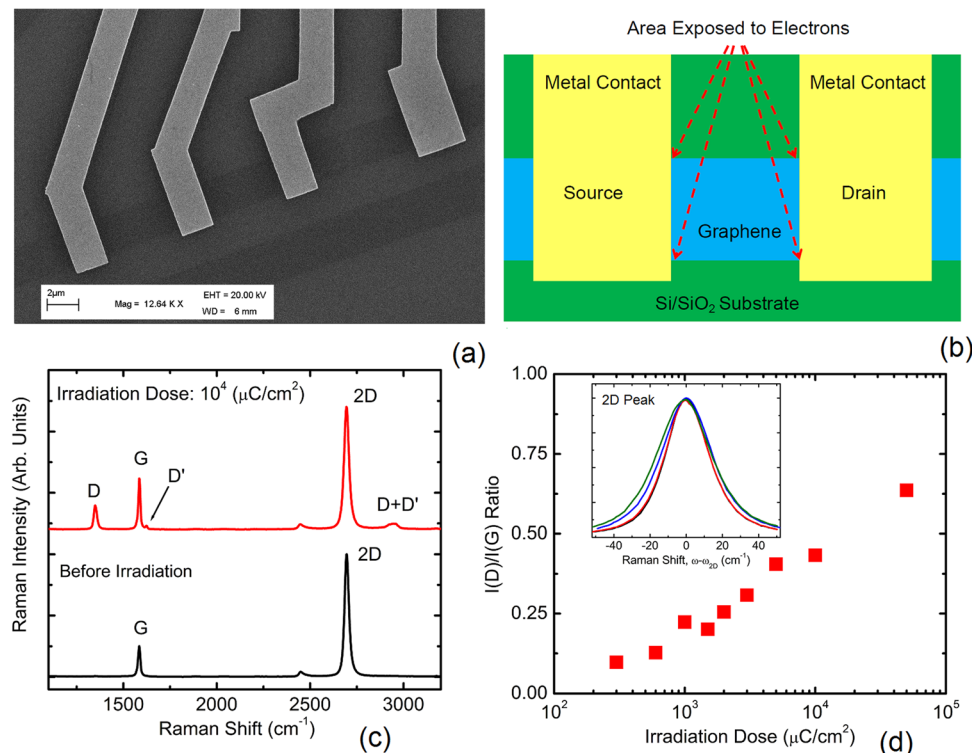


FIG. 1. Graphene device irradiation with electron beams. (a) SEM image of graphene devices with multiple metal contacts. The dark ribbons are graphene channels while the white regions are Ti/Au(10-nm/90-nm) electrodes. The scale bar is 2 μm . (b) Schematic of the irradiation process showing the area exposed to the electron beam. The whole area between the metal contacts is irradiated. (c) Raman spectrum of graphene before and after irradiation. The single-layer graphene signatures include G peak at $\sim 1584 \text{ cm}^{-1}$ and symmetric 2D band at $\sim 2692 \text{ cm}^{-1}$. The absence of the disorder D peak at $\sim 1350 \text{ cm}^{-1}$ proves that graphene is high quality and defect-free before irradiation. Appearance of the disorder D and D' peaks after irradiation indicates that electron bombardment introduced defects to graphene. (d) Intensity ratio $I(D)/I(G)$ as a function of the irradiation dose. The inset shows the normalized 2D band at different irradiation doses shifted in energy to the same position for the ease of comparison. Note the asymmetric broadening and skewing toward the lower wave numbers. The full-width at half maximum of 2D band before irradiation was $\sim 28 \text{ cm}^{-1}$ while after irradiation it increased to $\sim 36 \text{ cm}^{-1}$ at the irradiation dose of $5 \times 10^4 \mu\text{C}/\text{cm}^2$.

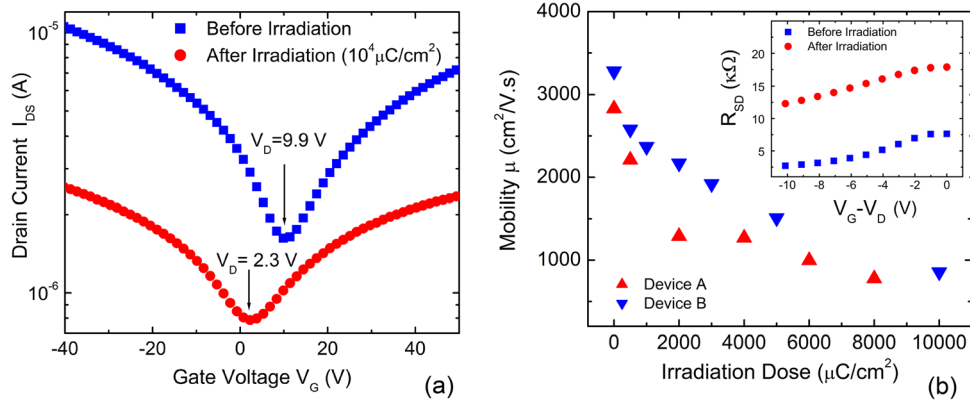


FIG. 2. Irradiation effects on electrical characteristics of graphene. (a) Source-drain current as a function of the back-gate bias. The position of the Dirac point shifts to a smaller voltage as a result of irradiation. (b) Electron mobility dependence on the irradiation dose for two devices. The mobility values for the pristine devices were in the range from 2500 to 5000 cm^2/Vs at room temperature. The inset shows a corresponding increase of the graphene channel resistance after irradiation for one of the devices. The initial areal irradiation dose of $300 \mu\text{C}/\text{cm}^2$ is comparable to the typical dose of $500 \mu\text{C}/\text{cm}^2$ in the lithographic process.

ground potential. Voltage fluctuations from the drain load resistance of $R_L = 10 \text{ k}\Omega$ were analyzed with the dynamic signal analyzer. Details of the measurements were described by us elsewhere.^{10,14}

Figure 3(a) shows the noise amplitude $A = (1/N) \sum_{m=1}^N f_m S_{I_m} / I_m^2$ as a function of the gate bias and the channel resistance in pristine graphene. Note that the noise amplitude is a metric similar to the normalized noise spectral density, S_I/I^2 , but involves averaging over several frequencies. Its behavior is in agreement with the previous reports indicating that the noise characteristic of our devices were typical for graphene.^{9–15} Figure 3(b) presents the noise spectral density, S_I/I^2 , for a graphene device before irradiation and after each irradiation step. S_I/I^2 remains of $1/f$ -type before and after irradiation. The most surprising observation from Figure 3(b) is that the noise level in graphene *decreases* after irradiation. The outcome was *reproducible* as proven by repeating the measurements for a large number of devices (>20). Figures 4(a) and 4(b) show that the noise reduces monotonically with the increasing RD for the entire range of negative gate-bias voltages, $V_G - V_D$. The same trend was observed for the positive gate bias.

Since the electron mobility decreases with irradiation (Figure 2(b)), our results indicate the $1/f$ noise reduction with decreasing mobility. This is an opposite trend compared to those observed in many different materials. The flicker $1/f$

noise in semiconductors and metals is usually associated with structural defects. Therefore, introduction of defects by electron, ion, gamma, or X-ray irradiation normally results in increased levels of $1/f$ noise and reduced mobility.^{2,25–27} The decrease of the $1/f$ noise with increasing mobility was also reported in graphene.¹³ The later results were interpreted using the modified Hooge relation. The different noise behavior in our case can be attributed to different nature of the mobility limiting mechanisms in the irradiated graphene samples.

Although the reduction of $1/f$ noise after irradiation is unusual for conventional materials, it is not unprecedented. There have been several reports when the $1/f$ noise decreased as a result of irradiation.^{31,32} In all previously reported cases of the $1/f$ noise reduction—a specific mechanism was responsible for the observed effect. Often, it was related to a particular device design.^{31,32} In our investigation, we employed the simplest device structure—a generic graphene channel with a back-gate for controlling the number of carriers. It appears that the noise reduction phenomenon in graphene is of more general nature related to the specifics of the electron transport as discussed below.

Without drawing conclusions on the dominance of a specific mechanism or mechanisms, it is illustrative to consider the limiting cases of $1/f$ noise originating from the fluctuations of the number of carriers vs. the fluctuations of the charge-carrier mobility. In semiconductors and transistors,

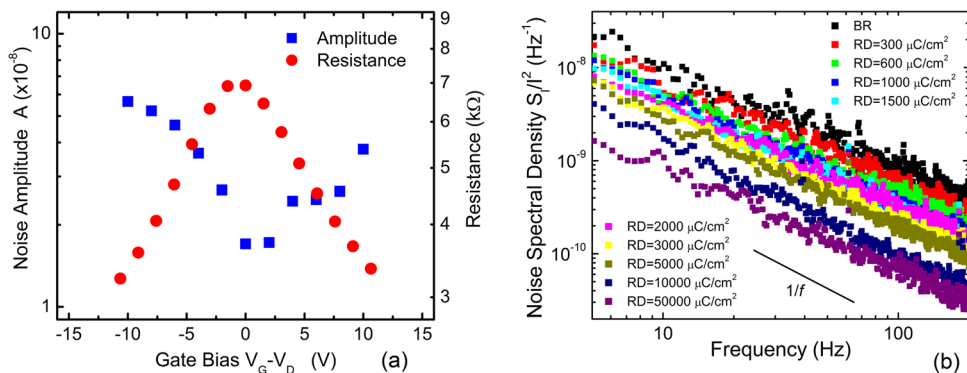


FIG. 3. Noise suppression in graphene via electron beam irradiation. (a) Noise amplitude A as the function of the gate bias and channel resistance in pristine graphene. (b) Noise spectral density, S_I/I^2 , as a function of frequency for a graphene device shown after each irradiation step. The source-drain DC bias was varied between 10 mV and 30 mV during the noise measurements. Note that the $1/f$ noise *decreases* monotonically with the increasing irradiation dose. S_I/I^2 is more than an *order-of-magnitude* smaller after $5 \times 10^4 \mu\text{C}/\text{cm}^2$ radiation does than that in pristine graphene.

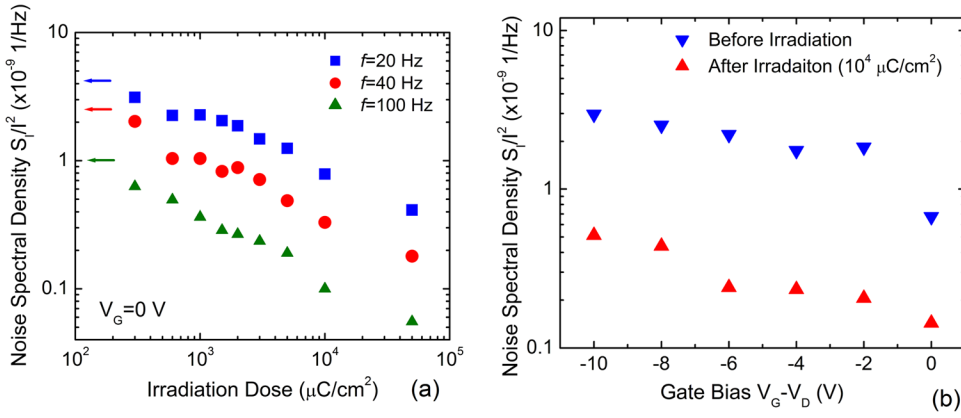


FIG. 4. Mechanism of the noise suppression in graphene. (a) S_I/I^2 as a function of the radiation dose at zero gate bias for three frequencies $f=20, 40,$ and 100 Hz. The arrows indicate the level of $1/f$ noise before irradiation. (b) S_I/I^2 as a function of the gate bias, V_G , referenced to the Dirac point, V_D , for another graphene device before and after irradiation plotted for $f=20$ Hz. The negative bias corresponds to the hole-transport regime. Note that the noise suppression in graphene via defect engineering works in the entire range of biasing conditions and frequencies pertinent to practical applications.

$1/f$ noise usually complies with the classical McWhorter model of the number of carriers fluctuations.³³ In this model, $1/f$ spectrum is a result of superposition the electron trapping and de-trapping events mediated by tunneling to the oxide traps located at difference distances from the channel. Since the tunneling probability depends exponentially on the distance between a trap and the channel, there is an exponentially wide distribution of the characteristic times, τ . A wide distribution of τ results in the $1/f$ overall noise spectral density written as^{34,35}

$$\frac{S_I}{I^2} = \frac{\lambda k T N_t}{f A_0 V n^2}. \quad (1)$$

Here, N_t is the concentration of the traps near the Fermi level responsible for noise, A_0 is the gate area, n is the carriers concentrations, and λ is the tunneling constant.

One can see from Eq. (1) that the only way to explain the noise reduction within the number-of-carriers fluctuation mechanism is to assume the decrease in N_t as a result of irradiation. Figure 2(a) shows that the Dirac point shifts to a smaller positive value after irradiation. Therefore, for the same gate voltage, the Fermi level position is different in the pristine and irradiated samples. Since the maximum contribution to the noise comes from the traps located near the Fermi level, the reduction of noise is not prohibited in the framework of the McWhorter model. However, the overall gate-voltage dependence of noise does not comply with the McWhorter model. While McWhorter model predicts $1/n^2$ dependence of noise, experiments with graphene show a variety of dependences including weak decrease or increase of noise with the gate voltage, i.e., with the concentration n .⁹⁻¹⁵ The above scenario also leads not only to decrease of noise at some gate bias but also to increase of the noise at other gate bias. We have not observed an increase in noise at other gate biases. However, the latter can be due to the fact that several mechanisms are responsible for the noise as discussed above.

In the framework of the mobility-fluctuation model, the noise spectral density of the elemental fluctuation events contributing to $1/f$ noise in any material is given by^{34,35}

$$\frac{S_I}{I^2} \propto \frac{N_t^\mu \tau \zeta (1 - \zeta)}{V} \frac{1}{1 + (\omega \tau)^2} l_0^2 (\sigma_2 - \sigma_1)^2, \quad (2)$$

where N_t^μ is the concentration of the scattering centers of a given type, l_0 is the mean free path of the charge carriers, ζ

is the probability for a scattering center to be in the state with the cross-section σ_1 . Integration of Eq. (2) results in the $1/f$ spectrum caused by the mobility fluctuations. One should note that N_t^μ is not a concentration of the scattering centers, which limit the electron mobility but rather a concentration of the centers contributing to the mobility fluctuations. The number of such centers may increase or stay unchanged as a result of irradiation. Indeed, there are many different types of scattering centers, which define the mobility and therefore the mean free path. After irradiation, the total number of these centers increases and, as a result, the mean free path decreases. However, not all types of the scattering centers contribute to $1/f$ noise. The characteristic frequency of the scattering cross section fluctuations for some of the centers can be out of the frequency band where the noise was measured (the scattering centers or traps can be either too slow or too fast). It is possible that the concentration of that particular type of scattering centers, which contribute to the mobility fluctuations either remains unchanged or only slightly increases. Therefore, the dependence on noise on the irradiation dose is mainly governed by the mean free path, l_0 . The mobility and, correspondingly, l_0 ($\sim \mu$) decrease as a result of irradiation (see Figure 2(b)) leading to the reduction in S_I/I^2 ($\sim l_0^2$). In graphene, μ is limited by the long-range Coulomb scattering from charged defects even at room temperature (RT),^{36,37} in contrast to semiconductors or metals, where μ at RT is typically limited by phonons, even if the defect concentration is high. Thus, it follows from our measurements and Eq. (2) that mobility-fluctuation mechanism can explain the noise reduction as a result of irradiation over the entire gate-bias range. Our results also suggest that the defects generated in graphene by irradiation are not the type of defects with the switching ionization because that would yield a normalized $1/f$ noise proportional to the mobility.³⁸

The noise reduction after irradiation came at the expense of the mobility degradation from the average value of $3000 \text{ cm}^2/\text{V s}$ to about $1000 \text{ cm}^2/\text{V s}$ at RT. Irradiating the device with the higher initial mobility ($\mu = 5000 \text{ cm}^2/\text{V s}$) with the same RD resulted in $\mu \sim 2000 \text{ cm}^2/\text{V s}$, consistent with the prior mobility studies.³⁹ This reduction in mobility although substantial does not preclude practical applications. It has been noted that for graphene devices used in nanometer-scale architectures the mobility above $\sim 1000\text{--}1500 \text{ cm}^2/\text{V s}$ is not even needed owing to the onset of the ballistic transport regime when the source-drain distance shrinks to the deep-submicron limit.⁴⁰ The same approach for

noise reduction can be potentially used for the devices with the channels implemented with graphene multilayers. It was recently demonstrated that $1/f$ noise in graphene multilayers is dominated by contributions from the surface—graphene layer in contact with the substrate—in the channels with the thickness of up to about seven atomic planes.⁴¹

In conclusion, we found that $1/f$ noise in graphene reduces upon introduction of defects via the low-energy electron-beam irradiation. The noise reduction comes at the expense of the mobility degradation. However, there is a possibility of the trade-off since the mobility after irradiation still remains relatively high for practical applications. We anticipate that other types of irradiation can produce similar effects although the required energies and doses can be different. The described *defect engineering* technique can open up alternative routes to graphene radiation-hard applications in aviation, space, and medical fields.

The work at UCR was supported, in part, by the Semiconductor Research Corporation (SRC) and Defense Advanced Research Project Agency (DARPA) through STARnet Center for Function Accelerated nanoMaterial Engineering (FAME), and by the National Science Foundation (NSF) Project Nos. US EECs-1128304, EECs-1124733, and EECs-1102074. The work at RPI was supported by the US NSF under the auspices of I/UCRC “CONNECTION ONE” at RPI and by the NSF EAGER program. S.R. acknowledges partial support from the Russian Fund for Basic Research (RFBR) Grant No. 11-02-00013.

¹I. Flinn, *Nature* **219**, 1356–1357 (1968).

²A. A. Balandin, *Noise and Fluctuations Control in Electronic Devices* (American Scientific Publishers, Los Angeles, 2002).

³K. S. Novoselov, A. K. Geim, S. V. Morozov, D. Jiang, M. I. Katsnelson, I. V. Grigorieva, S. V. Dubonos, and A. A. Firsov, *Nature* **438**, 197–200 (2005).

⁴Y. Zhang, Y.-W. Tan, H. L. Stormer, and P. Kim, *Nature* **438**, 201–204 (2005).

⁵Y. Wu, Y. M. Lin, A. A. Bol, K. A. Jenkins, F. Xia, D. B. Farmer, Y. Zhu, and P. Avouris, *Nature* **472**, 74–78 (2011).

⁶X. Yang, G. Liu, M. Rostami, A. A. Balandin, and K. Mohanram, *IEEE Electron Device Lett.* **32**, 1328–1330 (2011).

⁷F. Schedin, A. K. Geim, S. V. Morozov, E. W. Hill, P. Blake, M. I. Katsnelson, and K. S. Novoselov, *Nature Mater.* **6**, 652–655 (2007).

⁸S. Rumyantsev, G. Liu, M. Shur, R. A. Potyrailo, and A. A. Balandin, *Nano Lett.* **12**, 2294–2298 (2012).

⁹Y. M. Lin and P. Avouris, *Nano Lett.* **8**, 2119–2125 (2008).

¹⁰S. Rumyantsev, G. Liu, W. Stillman, M. Shur, and A. A. Balandin, *J. Phys.: Condens. Matter* **22**, 395302 (2010).

¹¹G. Xu, C. M. Torres, Jr., Y. Zhang, F. Liu, E. B. Song, M. Wang, Y. Zhou, C. Zeng, and K. L. Wang, *Nano Lett.* **10**, 3312–3317 (2010).

¹²I. Heller, S. Chatoor, J. Mannik, M. A. G. Zevenbergen, J. B. Oostinga, A. F. Morpurgo, C. Dekker, and S. G. Lemay, *Nano Lett.* **10**, 1563–1567 (2010).

¹³Y. Zhang, E. E. Mendez, and X. Du, *ACS Nano* **5**, 8124–8130 (2011).

¹⁴G. Liu, S. Rumyantsev, M. Shur, and A. A. Balandin, *Appl. Phys. Lett.* **100**, 033103 (2012).

¹⁵A. A. Kaverzin, A. S. Mayorov, A. Shytov, and D. W. Horsell, *Phys. Rev. B* **85**, 075435 (2012).

¹⁶A. A. Balandin, *Nature Mater.* **10**, 569–581 (2011); D. L. Nika and A. A. Balandin, *J. Phys.: Condens. Matter* **24**, 233203 (2012).

¹⁷S. L. Rumyantsev, N. Pala, M. S. Shur, R. Gaska, M. E. Levinshstein, M. A. Khan, G. Simin, X. Hu, and J. Yang, *J. Appl. Phys.* **90**, 310–314 (2001).

¹⁸A. N. Pal, S. Ghatak, V. Kochat, E. S. Sneha, A. Sampathkumar, S. Raghavan, and A. Ghosh, *ACS Nano* **5**, 2075 (2011).

¹⁹A. N. Pal and A. Ghosh, *Phys. Rev. Lett.* **102**, 126805 (2009).

²⁰E. Rossi, J. H. Bardarson, M. S. Fuhrer, and S. Das Sarma, *Phys. Rev. Lett.* **109**, 096801 (2012).

²¹E. H. Hwang, S. Adam, and S. Das Sarma, *Phys. Rev. Lett.* **98**, 186806 (2007).

²²T. Ando, *J. Phys. Soc. Jpn.* **75**, 074716 (2006).

²³K. Nomura and A. H. MacDonald, *Phys. Rev. Lett.* **96**, 256602 (2006).

²⁴J.-H. Chen, W. G. Cullen, C. Jang, M. S. Fuhrer, and E. D. Williams, *Phys. Rev. Lett.* **102**, 236805 (2009).

²⁵J. H. Scofield, T. P. Doerr, and D. M. Fleetwood, *IEEE Trans. Nucl. Sci.* **36**, 1946–1953 (1989).

²⁶D. M. Fleetwood, T. L. Meisenheimer, and J. H. Scofield, *IEEE Trans. Electron. Dev.* **41**, 1953–1964 (1994).

²⁷M. H. Tsai and T. P. Ma, *IEEE Trans. Nucl. Sci.* **39**, 2178–2185 (1992).

²⁸A. V. Krasheninnikov and F. Banhart, *Nature Mater.* **6**, 723–733 (2007).

²⁹D. Teweldebrhan and A. A. Balandin, *Appl. Phys. Lett.* **94**, 013101 (2009).

³⁰J. Kotakoski, D. S. Cottin, and A. V. Krasheninnikov, *ACS Nano* **6**, 671–676 (2012).

³¹J. P. Dubuc, E. Simoen, P. Vasina, and C. Claeys, *Electron. Lett.* **31**, 1016–1018 (1995).

³²S. Meskinis, G. Balcaitis, J. Matukas, and V. Palenskis, *Solid-State Electron.* **47**, 1713–1718 (2003).

³³A. L. McWhorter, in *Semiconductor Surface Physics*, edited by R. H. Kingston (University of Pennsylvania Press, Philadelphia, 1957), pp. 207–228.

³⁴Yu. M. Galperin, V. G. Karpov, and V. I. Kozub, *Sov. Phys. JETP* **68**, 648 (1989).

³⁵A. P. Dmitriev, M. E. Levinshstein, and S. L. Rumyantsev, *J. Appl. Phys.* **106**, 024514 (2009).

³⁶K. I. Bolotin, K. J. Sikes, Z. Jiang, G. Fundenberg, J. Hone, P. Kim, and H. L. Stormer, *Solid State Commun.* **146**, 351–355 (2008).

³⁷T. Stauber, N. M. R. Peres, and F. Guinea, *Phys. Rev. B* **76**, 205423 (2007).

³⁸L. B. Kiss and T. G. M. Kleinpenning, *Physica B* **145**, 185–189 (1987).

³⁹G. Liu, D. Teweldebrhan, and A. A. Balandin, *IEEE Trans. Nanotechnol.* **10**, 865 (2011).

⁴⁰P. Avouris, “Graphene electronics: Device physics and applications,” in Invited Talk, Symposium Y: Functional Two-Dimensional Layered Materials, Materials Research Society (MRS) Spring Meeting, San Francisco, California, USA (2011).

⁴¹G. Liu, S. Rumyantsev, M. Shur, and A. A. Balandin, *Appl. Phys. Lett.* **102**, 093111 (2013).